

DISCRETE GREEN FUNCTIONS APPROACH TO PREDICT CONVECTIVE HEAT TRANSFER

David G. Cuadrado
Purdue University
Indiana, United States

Guillermo Paniagua
Purdue University
Indiana, United States

ABSTRACT

The characterization of the convective heat transfer process should preferably be based on invariants descriptors independent from the thermal boundary conditions. The convective heat transfer has been traditionally expressed using the convective heat transfer coefficient included in the Newton's law of cooling. Regrettably, this coefficient depends on the actual flow temperature due to the temperature dependence of the viscosity. Hence, unsteady thermal boundary conditions would result in a varying convective heat transfer coefficient. To resolve this challenge, the adiabatic heat transfer coefficient [1] and the Green Function approach [2] were proposed to identify a convective heat transfer invariant from the thermal boundary conditions.

In this paper we propose the use of the Discrete Green Function (DGF) coefficients to characterize a backward-facing step. The complex flow topology exhibits regions of separation, recirculation and reattachment. The analysis is completed with the evaluation of the effect of different inlet boundary conditions in the DGF coefficients.

NOMENCLATURE

Symbol	Meaning [units]
A	Area [m^2]
DGF	Discrete Green's Function
G	Discrete Green's function coefficient
G^{-1}	Inverse Discrete Green's function coefficient
g	Green's function coefficient
h	Convective heat transfer coefficient [$\text{W}/\text{m}^2\text{-K}$]
k	Thermal Conductivity [$\text{W}/\text{m-K}$]
Nu	Nusselt number [-]
Pr	Prandtl number [-]
Re	Reynolds number [-]
St	Stanton number [-]
\dot{q}_{conv}	Convective heat transfer flux [W]
T	Temperature [K]

INTRODUCTION

In turbine applications, the extreme thermal and mechanical conditions limit the operation of sensors as well as the optical access. Therefore the convective heat transfer coefficient is usually defined using far field temperature data. However, the thermal boundary conditions within the model typically change in time and space, hence the conventional Newton law approach based on the upstream total temperature and local surface temperature is not adequate to define an invariant descriptor.

The Green Function approach delivers an array of different coefficients associated to the aerodynamic conditions, dictated by the geometry. Such array is independent of the thermal inlet conditions. The controlled surface is discretized into cells and each cell is associated to a vector of coefficients. The Discrete Green Function coefficients are calculated using the temperature response of the cell to a heat flux pulse imposed at different locations.

The Green Function approach has been applied by Moffat [2] using the superposition technique to analyze conductive heat flux along electronic cooling systems. Vick et al. [3] calculated the convective heat transfer problem for flow in tubes with non-uniform boundary conditions. Batchelder and Eaton [4] assessed the heat transfer through a turbulent boundary layer imposing uniform heat flux. Booten and Eaton [5] applied this methodology to assess heat exchange in the internal cooling passages of a turbine blade [6].

In this paper we study a backward-facing step. Aerodynamically, the backward-facing step offers different regions where the behavior of the convective heat flux cannot be interpolated and therefore we have performed a full analysis of the wall heat exchange.

METHODOLOGY

The definition of the convective heat transfer has been historically expressed by Newton's law of cooling which is expressed as:

$$h = \frac{\dot{q}_{conv}/A}{T_{flow} - T_{surface}} \quad (1)$$

The convective heat transfer coefficient is the ratio between the convective heat flux and the flow to surface temperature difference. In transient or unsteady conditions the coefficient is not constant since the flow to surface temperature difference keeps constant while a change in the heat flux is measured due to the fluctuating boundary layer. In order to extend the definition to complex flows with non-uniform and varying boundary conditions, we should broaden the evaluation of a new convective heat transfer coefficient that keeps the linearity in the concept. Therefore, if a change in temperature occurs ($T_{flow} - T_{surface}$) this should represent a proportional change in the heat transfer rate. The linearity of the energy equation can be applied with a superposition technique to measure the data extracted from the flow simulation developed in Fluent and determine the Green's function distribution for this specific case of study.

In linear differential equations the principle of superposition is often applied. In this paper the Green's function method is applied to determine the relationship between convective heat flux and the surface temperature field. In a first approximation the energy equation is linearized for the convective heat transfer, which limits the applicability to small temperature differences [2]. The Discrete Green's Function (DGF) was applied to predict the heat transfer over a backward-facing step with a constant heat flux applied to the bottom plate.

The region is discretized into n strips, each with a different length l . l is smaller close to the corner where the recirculation is expected. l increases along the axial distance (x). The rise in temperature is thereafter discretized in different pulses representing the average increase of temperature for each strip as shown in Figure 1. The resulting heat flux distribution is integrated over each strip to obtain the discretized heat rate distribution.

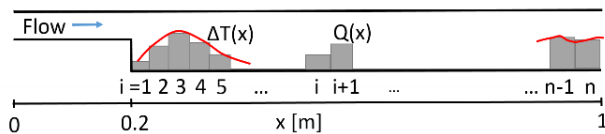


Figure 1. Surface discretization approach.

In order to accurately calculate the coefficients that define the heat flux and the associated increment of temperature at the wall, an isothermal calculation has been performed. The discretization of the bottom plate is based in this calculation. This isothermal calculation was performed with ambient

temperature on the walls and a flow temperature 100K higher.

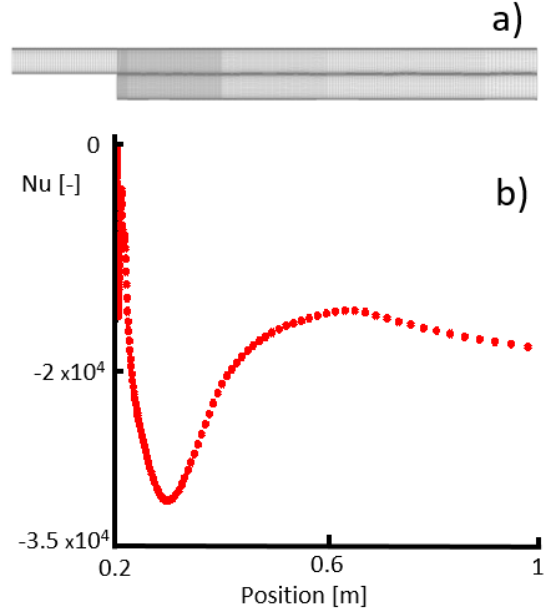


Figure 2. a) Numerical domain. b) Nusselt number for isothermal wall conditions.

The Discrete Green's Function, G , is the matrix that defines a relationship between the distribution of the discrete temperature rise and the corresponding distribution of discretized heat rate. It can be written as an array of elements such as:

$$\dot{q}_{ij} = g_{ij}\Delta T_j, \quad (2)$$

where g_{ij} is the element of G relating the average temperature rise on strip j and the resulting heat rate on strip i . The superposition technique considers individually the effects of each of the n square pulses in temperature rise. The net effect on element i is the summation of all n elements, such as:

$$\dot{q}_i = \sum_{j=1}^n g_{ij}\Delta T_j \quad (3)$$

Or in matrix form:

$$\dot{q} = G\Delta T \quad (4)$$

where ΔT is the vector containing the discrete temperature rise at each step and \dot{q} is the vector containing the heat rates. Each pulse in temperature rise along the domain affects the resulting heat rate at any location. The inverse Discrete Green's Function, G^{-1} , relates the heat rate distribution to a

temperature rise distribution, a matrix of dimension equal to G . Each element of the matrix fulfills [4]:

$$\Delta T_{ij} = g_{ij}^{-1} \dot{q}_j \quad (5)$$

Using the method of superposition the total temperature rise response can be written in terms of a matrix multiplication

$$\Delta T = G^{-1} \dot{q} \quad (6)$$

In order to obtain the temperature distribution, 2D RANS calculations were performed using ANSYS Fluent and imposing pulses of heat flux at each discretized strip. The simulations have been performed using Realizable k-epsilon turbulence model without wall functions. The analyzed geometry is observed in the Figure 2a) and the bottom plate is located between the axial position 0.2m and 1m. The baseline calculation was performed at ambient pressure, with a flow inlet temperature of 400K and an initial wall temperature of 300K. The inlet Mach number was selected as 0.12.

The heat flux q_{i1} is applied imposing 10000 W/m² in each strip. The 2D RANS simulation allow to retrieve the temperature distribution ΔT_{ji} at every cell. The Green's Function G_{ij} defines the following relationship [4]

$$q_{i1} = G_{ij} \Delta T_{j1} \quad (7)$$

Where there are N^2 unknown elements in G_{ij} and N equations. Considering the heat transfer for a value of $M - 1$ temperature distributions it gives

$$q_{im} = G_{ij} \Delta T_{jm} \quad (8)$$

In all these calculations the ΔT must be referenced to a reference temperature. In turbines, the reference temperature is usually the turbine upstream temperature in the plane upstream of the studied vane or blade. In this work, the reference temperature used is the adiabatic wall temperature [6]. The adiabatic wall temperature differs significantly from the inlet total temperature, especially at higher Re numbers and when the local Mach number is higher than 0.2 [7]. Therefore this temperature has been extracted from another simulation without heat flux in the bottom plate. The temperature drop may be explained by the use of a recovery factor applied to the total temperature at the inlet.

$$\frac{T_0}{T_{adiabatic\ wall}} = 1 + r_c \frac{\gamma - 1}{2} Ma^2 \quad (9)$$

The recovery factor is based on empirical correlations for specific geometries [8]:

$$r_c \approx Pr^{1/3} \quad (10)$$

The use of this recovery factor is fundamental for cases with flow Mach number over 0.2, since the error in the determination of the coefficients become significant. In the analyzed case, the adiabatic wall temperature at high Mach numbers was determined by a simulation imposing adiabatic walls, since the recovery factor varies with the axial location in complex geometries with recirculation and reattachment.

The final discretization includes 42 strips, with 20 of them between the axial positions 0.2 and 0.4; 10 of them between 0.4 and 0.6; other 10 between 0.6 and 0.9 and the last two between 0.9 and 1m. In all these sectors, the strips are equal in length.

42 calculations were performed to determine the DGF coefficients. In these calculations, we imposed a pulse per length unit, since the length of the strips is variable depending on the sector, and we evaluate the associated change in temperature at every strip.

The coefficients are calculated using the equation (7) and the inputs of heat flux and increment of temperature obtained in the simulation. With these coefficients three different studies have been carried out at different inlet conditions.

NUMERICAL ASSESSMENT OF THE DGF

The validation of the Green Function approach has been performed using a prescribed heat flux distribution which is detailed in the Figure 3b). The validation consisted in a comparison of the temperatures calculated with the inverse method and the temperature at the wall obtained using 2D RANS calculations with ANSYS Fluent.

In Figure 3c) the agreement between the result obtained with the DGF approach and CFD results is represented. There is a noticeable disagreement in the section next to the vertical wall. There are different reasons for this difference. The existence of a secondary vortex in this part may affect the calculations if the aerodynamic phenomena is not exactly the same in all the analyzed cases, even though the steady state simulation is totally converged. Furthermore, in the simulations performed with the pulses, the temperature in this region gets very high values which can lead to a non-linearity in the results, since the air properties are affected by the heating pulse. The DGF approach is valid for linear equations and an improvement in the equations, using a linearization method must be applied in order to improve the results in this region of the geometry.

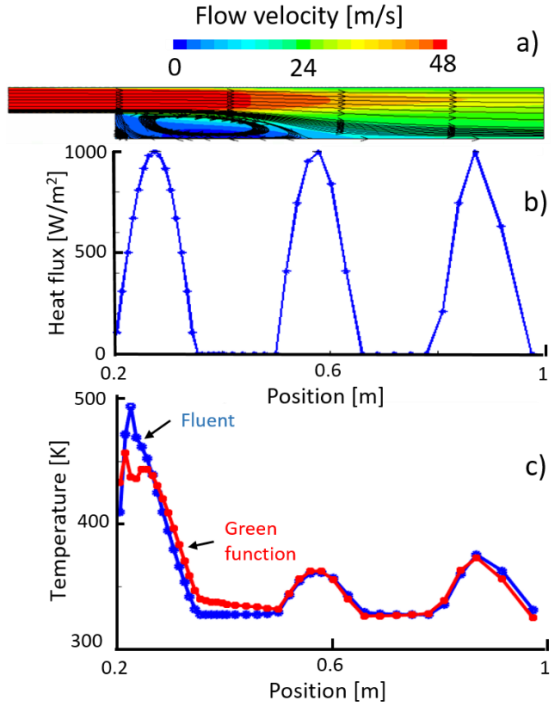


Figure 3. a) Backward-facing step geometry analyzed. b) Velocity field in the backward-facing step calculated with Ansys Fluent. c) Heat flux distribution used for the validation of the DGF approach.

The imposed heat flux is positive sinusoidal and it has been implemented in the bottom surface of the backward-facing step. The amplitude of the pulse is 1000 W/m^2 and follows a sinusoidal distribution. As stated, the area varies depending on the discretization and therefore the imposed heat rate at each surface varies as well.

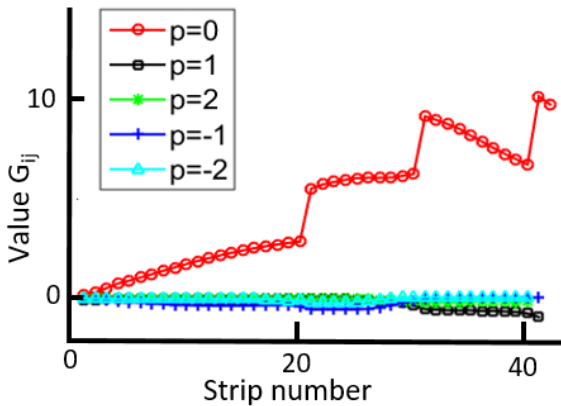


Figure 4. Values of the DGF coefficients in the main diagonal, sub-diagonals and super-diagonals of the Green Function matrix for the baseline case.

The different area of the discretization must be accounted in the calculation since the pulse is in Watts and in the Discrete Green Function matrix must appear this change in the area in order to avoid discontinuities in the calculation of the temperature at the wall. This is the reason of the steps in the values of the main diagonal coefficients of the DGF matrix represented in Figure 4. The representation of the main diagonal is fundamental to understand the behavior of the heat transfer along the bottom surface.

If we neglect the steps in the values where the heat rate provided from the surface has change, we can observe that the heat flux increase in the region where the recirculation bubble is located and achieves the maximum at the stagnation point. Downstream of the stagnation point the value of the main diagonal decreases due to the development of the boundary layer.

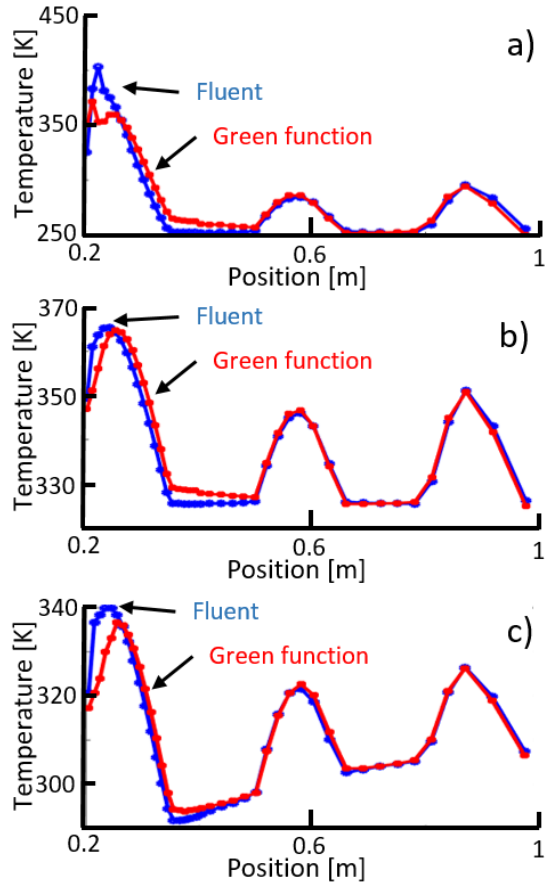


Figure 5. a) Comparison between CFD and DGF approach at 250K. b) Comparison between CFD and DGF approach at 4 bar. c) Comparison between CFD and DGF approach at Mach 0.85.

Figure 4 presents two superdiagonals and two subdiagonals, which represent the temperature effect of an imposed heat pulse in the adjacent strips to the analyzed strip. We can observe that they are close to 0, but its sign changes depending on the direction of the flow. Therefore in the stagnation point we observe that the line corresponding to the superdiagonal ($p=+1$) and the one corresponding to the subdiagonal ($p=-1$) are crossed. This means that the convection phenomena is mainly carried out due to the adjacent strip due to the velocity of the flow.

The methodology has been validated for different conditions of temperature, pressure and velocity represented in the (put reference of the next figures), where we can observe a good agreement for inlet flow temperature of 250K (Figure 5a)) and for an inlet pressure of 4bar (Figure 5b)).

At Mach numbers greater than 0.3 the equation (9) based in the recovery factor obtained using the equation (10) is unpractical. For complicated geometries, the range of Mach numbers in the recirculation and reattachment zone is large and the estimation of the adiabatic wall temperature must be based in the local Mach number.

INFLUENCE OF REYNOLDS NUMBER AND SURFACE TEMPERATURE

Different boundary conditions have been applied in order to validate the results in all possible conditions of velocity, pressure and temperature at the inlet of the domain. The effect of the different conditions in the value of the DGF coefficients and in the calculation of the Nusselt and Stanton number is represented in the figures displayed in this section.

The main objective of the DGF approach is to eliminate the dependence of the convective descriptor from the upstream temperature. In the Figure 6a), we can observe the independence of the value of the main diagonal DGF matrix calculated at different inlet total temperatures with the same conditions of pressure and velocity. It shows a good agreement in these values having a noticeable different where the velocity is higher in the outlet of the domain.

The Nusselt and the Stanton number are calculated using the inverse array of coefficients G^{-1} [5]. To compare the data with the literature obtained these dimensionless numbers must be defined based in the heat flux applied and the increment of temperature associated at each axial location. The increase of temperature related to a constant heat flux boundary is expressed by equation (6), where \dot{q} is the heat flow vector defined with as many constant values \dot{Q} as strips there are in the geometry. Then, the local Nusselt number is defined from

$$Nu_i = \frac{\left(\frac{\dot{Q}}{\Delta T_{j1}}\right)L}{k} \quad (11)$$

Where k is the thermal conductivity of the air and the considered characteristic length is the double of the size of the step [6]. The Stanton number also is defined locally using the previously calculated local Nu number, Re number and Pr number. Both Re and Pr numbers are calculated with the conditions at the inlet of the geometry.

$$St_i = \frac{Nu_i}{Re Pr} \quad (12)$$

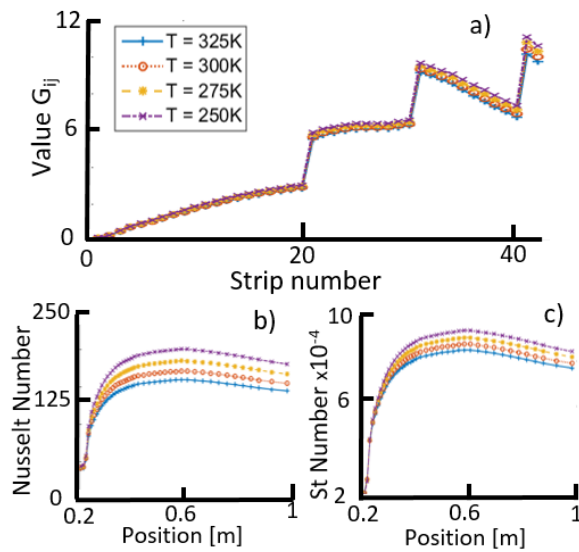


Figure 6. a) Comparison of the values of the DGF coefficients of the main diagonal at different inlet total temperatures. b) Comparison of the local Nusselt number at different inlet total temperatures. c) Comparison of the local Stanton number at different inlet total temperatures.

The local Nusselt and Stanton numbers calculated with the use of the DGF as explained in the equations (11) and (12) are presented in the Figure 6b) and Figure 6c). The values and distribution of these dimensionless numbers along the axial direction correspond with the expected trends found in the literature. The Stanton number and Nusselt number have the same trends in this case where the upstream temperature is modified, decreasing with the increase of temperature.

Different inlet pressure conditions have been evaluated as well. In this case, the different inlet properties do introduce a difference in the value of the coefficients of the main diagonal. As the pressure increase the value increase as well in an almost linear manner.

Regarding the effect on the local Nusselt and Stanton number, in this case they do not follow the same trends since the Re number is modified in a different rate that in the previous case. Therefore, while the local Nusselt number increase with the pressure, the local Stanton number has the opposite trend. This is due to the increase of Re number due to the increase of pressure. The Stanton number relates the effect of the local shear force at the wall, due to viscous drag, to the total heat transfer at the wall, hence if the Re number increases, the viscous drag increases and the ratio decreases.

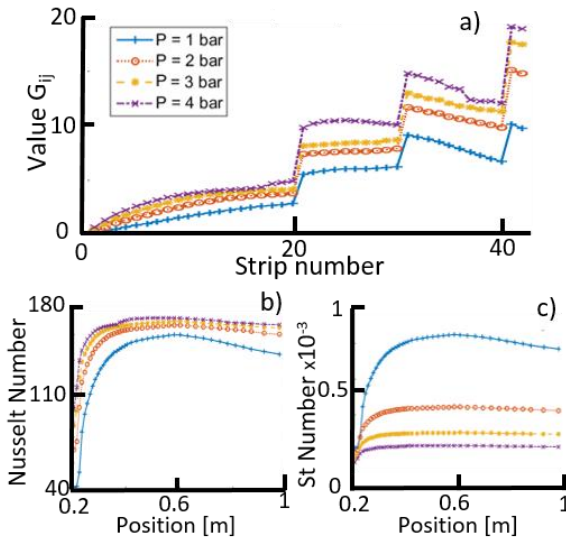


Figure 7. a) Comparison of the values of the DGF coefficients of the main diagonal at different inlet total pressures. b) Comparison of the local Nusselt number at different inlet total pressures. c) Comparison of the local Stanton number at different inlet total pressures.

The aerodynamic phenomena and the behavior of the flow has been changed also to know the effect of an increase in velocity in the calculation of the coefficients. The first important conclusion we can extract is the impossibility of using the same recovery temperature in the whole surface, since the Mach number in most of the regions exceeds 0.2. Therefore in order to get an accurate validation of the case at different velocities we need to define a local velocity which will lead to the definition of a local recovery temperature.

If we observe the values of the coefficients after applying the recovery temperature approach [6] we observe that the trends are similar to the ones found with the modification of the pressure, hence the Stanton and Nusselt numbers trends have similar behaviors as well. Only in the final part of the geometry, where the velocity is modified in a larger way amongst all the analyzed cases, the heat transfer phenomena varies. In the case of a Mach number

equal to 0.85, the trend in the downstream region is different since the reattachment has not happened yet at the outlet of the domain. In the upstream part near the vertical wall of the step, the behavior is similar in all conditions.

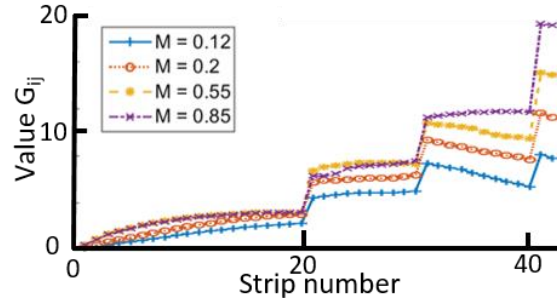


Figure 8. Comparison of the values of the DGF coefficients of the main diagonal at different Mach numbers.

NUMERICAL UNCERTAINTY

Mathematically, the process described as the Green function approach uses the imposition of an infinite magnitude of heat flux in an infinitesimal region, known as Dirac delta function. Physically and experimentally, this function must be approximated defining an area of application and a magnitude of the heat flux pulse.

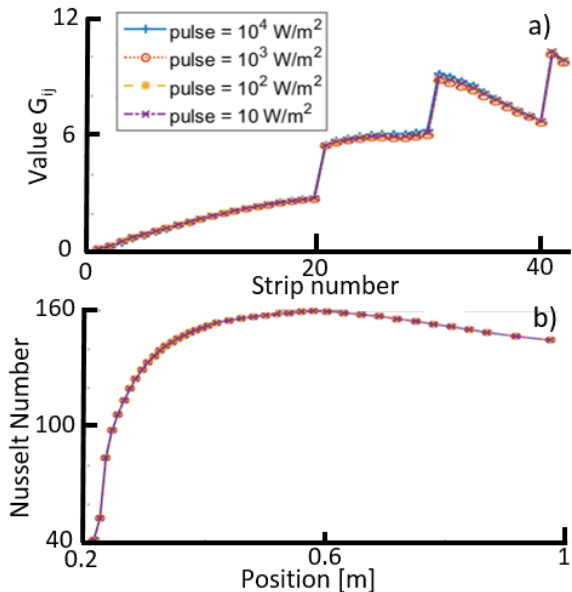


Figure 9. a) Comparison of the values of the DGF coefficients of the main diagonal with different magnitudes of heat flux pulse. b) Comparison of the local Nusselt number with different magnitudes of heat flux pulse.

The uncertainty of the calculations by imposing different values of impulse has been evaluated by

calculating the sensitivity of the value of the coefficients to a variation of the heat flux pulse. In Figure 9a) are represented the values of the main diagonal of the DGF matrix calculated imposing four different magnitudes of the pulse. There is a good agreement between all of them, but there are differences next to the reattachment of the flow. The objective of this section is to evaluate how sensitive the calculation is to the magnitude of the pulse.

Also it has been represented the effect of the pulse value variation in the Nusselt number calculation. In Figure 9b) the local value is represented, and it can be observed that following the procedure described in this work to calculate the local Nusselt number the value it is independent on the value of the pulse magnitude.

To analyze the sensitivity of the values to the magnitude of the pulse, we have modified the pulse by 1 unit in the different cases. Therefore we have estimated that the uncertainty in the imposed heat flux is 0.0001 W/cm^2 . In Figure 10, it is represented the sensitivity in percentage of the value of the main diagonal when you apply a pulse of 1 W/cm^2 and a pulse of 0.001 W/cm^2 . We can observe that the values with the smaller pulse have an average sensitivity near the 3% while with a higher pulse it is negligible. The calculated value on the average sensitivity is lower than $10^{-3} \%$. The regions where the velocity is smaller, near the stagnation points present higher levels of sensitivity than the rest of the coefficients.

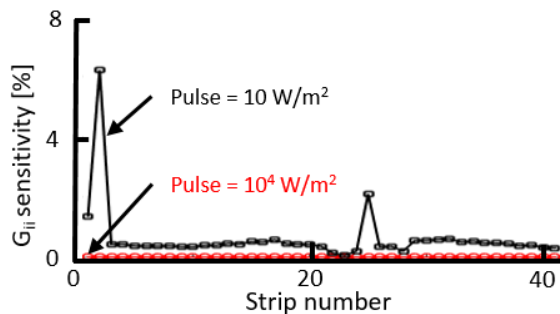


Figure 10. Comparison of the sensitivity of the DGF coefficients of the main diagonal due to the uncertainty in the heat flux pulse.

The accuracy in the calculation of the values of the matrix it is very important in order to be able to calculate the proper temperature distribution on a given case. When the pulse is higher, tending to an infinite value, the value of the coefficients is more accurate and therefore, we can introduce more uncertainty in the measurement of the adiabatic wall temperature used in the matrix calculation. If we combine the uncertainty in the measurement with a

small magnitude of the imposed pulse, the determination of the temperature distribution after applying the DGF approach would be shifted and therefore we would be unable to predict it.

If, instead of looking at the values of the DGF coefficients of the diagonals, we evaluate the uncertainty associated to the final calculation of the temperature given the DGF coefficients, we have to include the uncertainty associated to the temperature measurement. The highest level of uncertainty is provided by the increment of temperature associated to the heat pulse implementation. This increment is associated to both the precision in the definition of the adiabatic wall temperature and the magnitude of the pulse. Therefore, the uncertainty in the final temperature estimation due to the pulse is related to the temperature measurements. The smaller the magnitude of the pulse, the lower the increment of temperature.

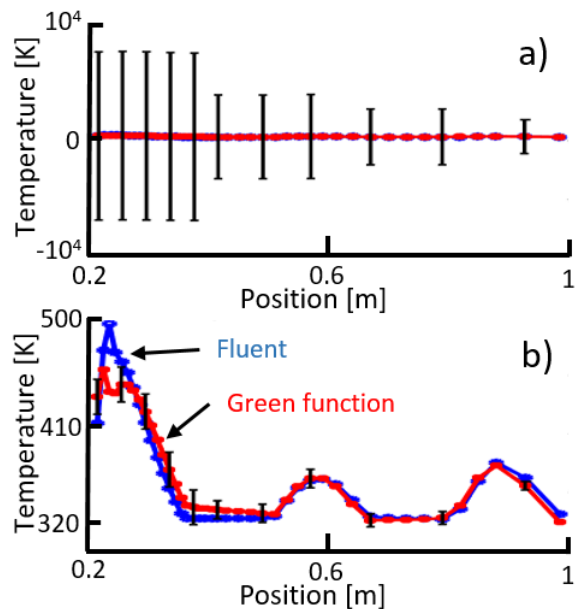


Figure 11. a) Uncertainty in the wall temperature estimation associated to a heat flux 10 W/m^2 and an uncertainty in the temperature measurement of 0.5 K . b) Uncertainty in the wall temperature estimation associated to a heat flux pulse of 10000 W/m^2 and an uncertainty in the temperature measurement of 0.5 K .

In Figure 11a) the uncertainty associated to a calculation using pulses of 10 W/m^2 and an uncertainty in the temperature measurement of 0.5 K is represented. As it can be observed the uncertainty in these temperature measurements is too high for the increment of temperature associated to the magnitude of the individual pulses, having an uncertainty over 500% in the point with less variation. In the Figure 11b) we can observe the

reduction of this uncertainty when we apply a pulse 1000 times larger. The uncertainty level of the estimation is reduced below the 5% for the same level of temperature uncertainty. Therefore the use of small magnitude pulses is impractical for the estimation of the wall temperature using the DGF methodology.

CONCLUSION

The Green Function coefficients are calculated as invariant descriptors of heat transfer phenomena in a backward facing step. These descriptors are obtained imposing heat flux pulses of the same magnitude at different spatial locations and evaluating their effect in change of temperature.

With this invariant matrix of coefficients we are able to predict the heat flux through a surface knowing the distribution of temperature over this surface. The results have been validated using CFD calculations performed with ANSYS Fluent in the same representative backward-facing step geometry.

Variations in the inlet temperature, inlet total pressure and the velocity of the flow have been introduced to evaluate their effect in the heat flux calculation method described in this paper.

The value of the heat flux pulse applied in the calculation of each one of the 42 temperature responses is another parameter that has been evaluated. The uncertainty of the calculation of the coefficients is mainly related to the value of these pulses. Moreover, there is a minimum value of heat flux pulse which may be experimentally (or numerically) applied in order to overcome the uncertainty associated to the measurement (or calculation) of the adiabatic wall temperature.

The two parameter associated to the uncertainty in the calculation are the measurement of the imposed heat flux in each one of the spatial locations and the adiabatic wall temperature calculated at the wall. It is observed that the uncertainty associated to the heat flux affects linearly the sensitivity of the coefficients. Therefore a 10% sensitive heat flux means 3% variation in the mean value of the green function coefficients at the diagonals and a 1% sensitivity in the heat flux means 0.3% variation in the DGF values of the diagonal. All calculations were performed with the same adiabatic wall temperature.

The uncertainty in the temperature measurements plays a significant role in the uncertainty of the calculations, being even more significant for smaller values of heat flux pulses. The use of small amplitude pulses is impractical for the estimation of the wall temperature due to the high uncertainty associated to the temperature measurements.

ACKNOWLEDGMENTS

The authors would like to acknowledge Mr. Tiago Reis for its collaboration in the first part of the project development and Prof. Marconnet for the advices during the work evaluation.

REFERENCES

- [1] Pinilla, V., Solano, J. P., & Paniagua, G. (2011, January). Method and Measurement of Adiabatic Wall Temperature Downstream of a High Pressure Turbine Using Thin-Film Sensors. In ASME 2011 Turbo Expo: Turbine Technical Conference and Exposition (pp. 1701-1708). American Society of Mechanical Engineers.
- [2] R. J. Moffat, "What's new in convective heat transfer?", *Int. J. Heat Fluid Fl.*, pp. vol. 19, no.2, pp. 90-101, Oct. 1997.
- [3] Vick, B., Beale, J. H., and Frankel, J. I., "Integral Equation Solution for Internal Flow Subjected to a Variable Heat Transfer Coefficient," *ASME J.*, vol. 109, no. No. 4, pp. pp. 856-860, 1987.
- [4] K. A. Batchelder and J. K. Eaton, "Practical Experience with the Discrete Green's Function Approach to Convective Heat Transfer," *J. Heat Transfer*, pp. vol. 123, no.1, pp. 70-76, May 2000.
- [5] Booten, C., and Eaton, J., 2005, "Discrete Green's Function Measurements in Internal Flows," *J. Heat Transfer*, 127, pp. 692-698.
- [6] Booten, C., and Eaton, J., 2007, "Discrete Green's Function Measurements in a Serpentine Cooling Passage," *J. Heat Transfer*, 129, pp. 1686-1696.
- [7] Elkins, C., Markl, M., Iyengar, A., Wicker, R., and Eaton, J., 2004, "Full Field Velocity and Temperature Measurements Using Magnetic Resonance Imaging in Turbulent Complex Internal Flows," *Int. J. Heat Fluid Flow*, 25, pp. 702-710.
- [8] White, F., 1991, *Viscous Fluid Flow*, 2nd ed., McGraw-Hill, New York.